Received: 7 March 2023 | Revised: 10 May 2023 | Accepted: 19 May 2023

DOI: 10.1096/fj.202300385R

METHOD

The FASEB Journal

Assessing *Acinetobacter baumannii* virulence and treatment with a bacteriophage using zebrafish embryos

Sofia Neto[1,2,3] | **Ana Vieira**[1] | **Hugo Oliveira**[2,3] | **Begoña Espiña**[1]

[1]International Iberian Nanotechnology Laboratory (INL), Braga, Portugal

[2]CEB—Center of Biological Engineering, University of Minho, Braga, Portugal

[3]LABBELS—Associate Laboratory, Guimarães, Portugal

Correspondence
Hugo Oliveira, CEB—Center of Biological Engineering, University of Minho, Rua da Universidade, Braga 4710-057, Portugal.
Email: hugooliveira@deb.uminho.pt

Begoña Espiña, International Iberian Nanotechnology Laboratory (INL), Av. Mestre José Veiga, Braga 4715-330, Portugal.
Email: begona.espina@inl.int

Funding information
European Regional Development Fund (ERDF), Grant/Award Number: NORTE-01-0145-FEDER-000047

Abstract

Acinetobacter baumannii is the leading bacteria causative of nosocomial infections, with high fatality rates, mostly due to their multi-resistance to antibiotics. The capsular polysaccharide (k-type) is a major virulence factor. Bacteriophages are viruses that specifically infect bacteria and have been used to control drug-resistant bacterial pathogens. In particular, *A. baumannii* phages can recognize specific capsules, from a diversity of >125 that exist. This high specificity demands the in vivo identification of the most virulent *A. baumannii* k-types that need to be targeted by phage therapy. Currently, the zebrafish embryo has particularly attained interest for in vivo infection modeling. In this study, an *A. baumannii* infection was successfully established, through the bath immersion of tail-injured zebrafish embryos, to study the virulence of eight capsule types (K1, K2, K9, K32, K38, K44, K45, and K67). The model revealed itself as capable of discerning the most virulent (K2, K9, K32, and K45), middle (K1, K38, and K67), and the less virulent (K44) strains. Additionally, the infection of the most virulent strains was controlled in vivo resorting to the same technique, with previously identified phages (K2, K9, K32, and K45 phages). Phage treatments were able to increase the average survival from 35.2% to up to 74.1% (K32 strain). All the phages performed equally well. Collectively, the results show the potential of the model to not only evaluate virulence of bacteria such as *A. baumannii* but also assess novel treatments' effectiveness.

KEYWORDS
Acinetobacter baumannii, bacteriophages, therapy, virulence, zebrafish embryo

1 | INTRODUCTION

Acinetobacter baumannii has become a major nosocomial pathogen that poses a particular threat in immunocompromised patients.[1,2] This bacterium has a high incidence among patients whose care requires devices such as ventilators, sutures, and catheters and causes wound, skin, lung, and bloodstream infections, which are particularly dangerous in intensive care units.[1,3]

A. baumannii is a leading bacterial pathogen for death associated with antibiotic resistance, killing over 500 000 people globally in 2019.[4] Many isolated strains are resistant to most, if not all, antibiotics.[5,6] In fact, many clinical isolates are already resistant to last-resort antibiotics, like

Abbreviations: CFU, colony forming units; dpf, days post fertilization; hpf, hours post fertilization; hpi, hours post infection; MOI, multiplicity of infection.

carbapenems, colistin, and third-generation cephalosporins.[7-11] As a result, *A. baumannii* has been designated by the World Health Organization as the number one priority pathogen for the development of novel antimicrobials.[7-11]

The capsule (k-type) is considered to be a major virulence factor of *A. baumannii*. This outer layer that surrounds bacteria is involved in intrinsic resistance to peptide antibiotics,[12] shields bacteria from host immune responses,[13,14] hides the receptors for predators (such as bacteriophages), and interacts with biotic and abiotic surfaces for biofilm formation, allowing environment adaptation.[15-17] As a consequence of many selective pressures, the capsule is highly diverse. The presence of at least 125 capsular forms in *A. baumannii* may indicate the complex and numerous defensive mechanisms established by this pathogen but the virulence and prevalence of the capsular types in clinical situations are unclear.[18,19] The first and only capsule typing technique has only recently (2020) become available through Kaptive.[20] Therefore, despite *A. baumannii* being associated with many nosocomial infections, links between particular capsule types and clinical infection remain poorly understood. Owing to the diversity of capsules, it is of utmost importance to establish novel methods capable of assessing the most virulent capsule types for epidemiology and targeted therapy.

Bacteriophages (phages) are viruses that infect bacteria but are harmless to human cells. Lytic phages, also known as virulent phages, recognize the host cells through specific receptors, inject their DNA inside the cells, and replicate the genetic material, leading to the synthesis of more lytic phage particles, lysing the cells in the end to release the progeny. Once the host cell is lysed, the virion finds a new host to infect and further replicate.[21-23]

Phage treatment has recently rekindled interest in handling difficult-to-treat bacterial infections. *Acinetobacter* phage therapy has already been assessed as an alternative to the non-functional antibiotics. In 2016, the first published medical intervention using phages was made to treat a systemic drug-resistant *A. baumannii* infection in the US, the well-publicized "Patterson case".[24] Since then, many *A. baumannii*-infecting phages have been isolated and characterized. Currently, there are several phages described that specifically recognize *A. baumannii* capsules through tail-spike proteins (K1-2, K9, K19, K27, K30, K32, K37, K44-45, K47-48, K87, K89, K91, K93, and K116).[18,25-28] Their antibacterial potential, however, has not been extensity tested in vivo. Worldwide, the zebrafish (*Danio rerio*) has become a popular non-mammalian vertebrate model for the study of infectious human diseases, due to the strong similarities of its innate immune system with that of humans, its unprecedented possibilities for real-time imaging, as well as the ease of maintenance, high fecundity, and rapid development.[29-31] Particularly, the use of embryos is receiving increasing attention, since they are considered as a replacement method for animal experiments for drug screening, with reduced ethical constraints.[31] Indeed, zebrafish embryo has now been used as a model to study pathogeny of diverse infections.[32] Moreover, *A. baumannii* infection has already been successfully established through systemic injection in zebrafish embryo.[32]

The chorion is the acellular coat that surrounds the embryo until the hatching period.[31,33] The embryo can either hatch naturally (starting at 48 h post-fertilization, hpf) or it can be removed artificially by resorting to enzymatic assistance or by mechanical dechorionation (starting at 6 hpf). The latter technique is quick, easy, and non-costly when perfected, and can be done in the early stages of development. After the natural or artificial hatching, the establishment of the infection and treatment delivery in the embryos can resort to two different pathways: microinjection or bath immersion.

Nogaret et al. (2021) have established a novel protocol for *Pseudomonas aeruginosa* infection in zebrafish embryo to assess the virulence of wild-type PAO1 and an attenuated mutant based on bath immersion of tail-injured embryo technique.[34] This study additionally validated the model for antipseudomonal drug testing with ciprofloxacin, a clinically validated antibiotic and a novel therapy confirmed in vitro but not in an organism model. Therefore, this novel protocol might serve as a base for establishing disease in zebrafish embryo with similar Gram-negative and opportunistic bacteria, such as *A. baumannii*, and later advancing for phage treatment.[34]

Although the phage antimicrobial therapy has already been successfully assessed for different pathogens, resorting to the zebrafish embryo model,[35,36] this therapy has only been performed through the systemic injection method, and never before with *A. baumannii* infections.

Consequently, the main goals of this work are to firstly implement the zebrafish embryo model of infection for *A. baumannii*, to later assess the virulence of different capsular types (K1, K2, K9, K32, K38, K44, K45, and K67). Another goal includes the evaluation of the effectiveness of phage therapy in controlling the infection in the zebrafish model. Hence, an additional goal is the selection and optimization of the therapy for the treatment of *A. baumannii* human disease, as a possible replacement for common non-functional antibiotics.

2 | MATERIALS AND METHODS

2.1 | Bacterial strains, phages, and media

A panel of eight different *A. baumannii* K-types (K1, K2, K9, K32, K38, K45, and K67), which belong to the collections of Alexandr Nemec (NIPH and ANC strains)

and of the Institute Pasteur (CIP 90 strains) or previously isolated by us, was used.[37] These strains were grown at 37°C in trypticase soy broth (TSB) or in trypticase soy agar (TSA, containing 1.2% agar). CHROMagar Acinetobacter was also used for Acinetobacter strains in the in vivo assays. Additionally, five phages specific for distinct *A. baumannii* capsule types (K1, K2, K9, K32, and K45 phages) previously available in the group were used for treatments.[19]

2.2 | Phage production

Acinetobacter phages were produced as previously described by Oliveira et al.[38] Phages were produced infecting mid-exponential growing strains (optical density OD600 of around 0.3) for 24 h at 37°C with agitation. Next, samples were centrifuged (4000 *g*, 15 min) and the supernatant was filtered (0.45-μm syringe filters). To purify phages, 1 g of PEG (Polyethylene Glycol 8000, Fisher BioReagents) was added for each 10 mL, followed by overnight incubation in a cold chamber (4°C, 120 rpm). The following day, samples were centrifuged (9500 *g* for 15 min, 4°C) and the pellet was resuspended in SM buffer (100 mM NaCl, 10 mM MgSO4, 50 mM Tris-HCl, pH 7.5). Subsequently, chloroform was added (1/4 of the volume of the suspension) for the removal of bacteria, and mixed with a vortex (Fisherbrand) for 1 min, followed by centrifugation (3500 *g* for 15 min, 4°C). Next, the upper translucent phase was collected and filtered (0.22 μm Whatman).

For phage titration, from the produced phage stock, 10-fold serial dilution was prepared in SM buffer. Next, 10 μL of each dilution was dropped and spread into the bacterial lawns, and incubated at 37°C overnight. The following day, plaque-forming units (PFU) were counted, and each phage stock's concentration was determined.

2.3 | Zebrafish embryos

2.3.1 | Adult zebrafish maintenance and breeding

Adult zebrafish from AB strain are maintained in 30-L aquariums with reconstituted freshwater. The aquarium is equipped with a thermometer, a heater, constant aeration, and a filter containing bio-balls, cotton, and active carbon. The water is kept at 26°C, with pH between 6.5 and 8, and a photoperiod of 14:10 (light: dark, L:D) is established. The fish are fed two times a day with tetra flakes ad libitum, and on breeding days with 48 h hatched *Artemia* sp.

For the egg production, 5:5 male-to-female ratio adult zebrafish were separated into breeding cages briefly before the start of the 10-h dark period. After 10 h, the light was turned on in order to start the mating. After 1 h of the onset of light, the fertilized eggs were collected, counted, and carefully washed with filtered freshwater (Thermo Scientific Nalgene Rapid Flow 50, 0.2 μm) multiple times. The embryos were maintained until 48 hpf at 28°C under standard conditions in filtered freshwater (0.05 g/L of NaCl, 0.03 g/L of $NaHCO_3$, and 0.003 g/L of $CaCO_3$); embryos were prepared with deionized water and filtered (Thermo Scientific Nalgene Rapid Flow 50, 0.2 μm). The dead embryos were discriminated by naked eye and removed, and the healthy embryos were kept in a Thermomixer (Eppendorf Thermomixer) at 28°C, until the dechorionation, tail wounding, and subsequent infection at 48 hpf.

2.3.2 | Zebrafish embryo bath immersion infection with *A. baumannii* and phage treatment

Bacterial strains newly streaked out of CHROMagar Acinetobacter plate stock were cultured in TSB medium at 37°C, 120 rpm, until 10^9 CFU/mL was attained, growing the culture up to an OD600 = 0.5 (NBI—Biotek Synergy H1 Microtiter Plate Reader). Bacteria were centrifuged for 15 min at 9000 rpm (Hettich Universal 320/320R centrifuge) and resuspended in filtered freshwater. After a second centrifugation, to guarantee proper TSB removal, the bacteria were suspended in freshwater at the correct concentration. The number of bacteria in the inoculum was then determined by subsequent plating onto CHROMagar Acinetobacter after dilution into PBS (Sigma-Aldrich). The initial bacteria concentration in each well was determined by averaging the CFU counting of three independent measurements.

Mechanical dechorionation was conducted on 48 hpf embryos, resorting to two sharp forceps and an illuminated digital microscope (Inskam Digital Microscope). The first forceps were used to grasp a single embryo's chorion while the other forceps gently tore the chorion without injuring the embryo. The dechorionated embryos were immediately placed in 24-well plates filled with 2 mL of filtered freshwater in the thermomixer, at 28°C, two embryos per well.

For the infection, two methods were tested:

2.3.2.1 | *Method 1*

The infection was then carried out on healthy 48 hpf embryos. Individually, and randomly picked, groups of 18 embryos were divided onto 96-well plates (TPP tissue culture plates with anti-condensation lid). All the unused wells were filled with up to 200 μL of freshwater

to ensure proper heat dispersion. For each strain, bacterial concentrations of 10^6, 10^7, 10^8, and 10^9 CFU/mL were tested. The plates were incubated at 28°C and kept under light. The number of dead embryos was obtained visually at certain time points under an illuminated digital microscope (Inskam Digital Microscope) based on the lack of heartbeat, for survival evaluation following infection. Anomalies in free swimming as well as the presence of malformations were also documented. The embryos were anesthetized with a room temperature anesthetic solution (Tricaine 0.4% (i.e., MS-222:ethyl 3-aminobenzoate methanesulfonate, Sigma-Aldrich), 99.34% Milli-Q water, and 0.26% Trizma base (Sigma-Aldrich, >99%) with adjusted pH 7.0, stored at −20°C) diluted 10X in freshwater and euthanized at 120 hpf. Additional controls were made to ensure that the embryo death was associated with the colonization of the bacteria: the negative control with no pathogen (consisting only of 200 µL of freshwater), and the heat killed/ethanol-killed bacteria suspensions. For the preparation of the heat-killed bacterial control, the bacteria suspended in filtered freshwater at the stated concentration was treated for 1 h at 65°C, which resulted in a 6-log fold drop in CFU/mL count. Regarding the ethanol-killed bacteria suspension, the inoculum was centrifuged and resuspended in ethanol 70% (CH_3CH_2OH, Chemlab) and incubated for 5 min. Then, to assure ethanol clearance, the bacteria were centrifuged twice more and resuspended in filtered freshwater to the required concentration.

2.3.2.2 | *Method 2*

Same as Method 1, but instead of healthy embryos, tail-injured embryos were used. To injure the tail fin prior to infection, embryos were placed in a Petri dish and anesthetized with the previously described room-temperature anesthetic solution. A scalpel blade was used to accomplish a minor transection of the tail (Surgeon carbon steel scalpel blades) under an illuminated digital microscope (Inskam Digital Microscope). The cut was performed crosswise at the beginning of the caudal vein, amputating the end of the tail, which was not included in the infection bath.For the treatment efficiency assessment, infected embryos were thoroughly washed at 12 hpi (hours post-infection) with freshwater to remove the bacteria. Then, the embryos were transferred to a new 96-well microtiter plate containing filtered freshwater supplemented with 10^9 PFU/mL (l0 µL) of the phage treatment, or the same volume of the treatment buffer or freshwater (controls). The embryos were then incubated at 28°C and for 2 days, monitored for mortality. When no heartbeat was detected in zebrafish embryos, they were deemed dead, being that opacification of the embryo was found to follow soon. Each experiment was conducted at least three times, and each condition within the experiment was assayed using 18 embryos.

2.4 | Data analysis

For the zebrafish embryo assay, the data from three separate trials were merged to analyze a total of 54 embryos for each group. For statistical analysis, GraphPad Prism 8 (GraphPad Software, San Diego, CA, USA) and Microsoft Excel (2013) were used. The log-rank test was used to make comparisons between survival curves. In the figures, * denotes a *p*-value of .05, ** a *p*-value of .01, and *** a *p*-value of .001.

2.5 | Ethics statement

All procedures described in this paper followed the standard operating procedures stablished at the International Iberian Nanotechnology Laboratory (INL) based on OECD guidelines for fish embryo acute toxicity (FET) test.[39] Adult zebrafish were not sacrificed for this investigation, as per the international norms stipulated by the EU Animal Protection Directive 2010/63/EU. According to the EU Animal Protection Directive 2010/63/EU, all studies were conducted prior to the embryos' free-feeding stage and did not fall under animal experimentation regulation. The existence of a heartbeat was employed as a clinical criterion for survival curves. Embryos were euthanized with a fatal dosage of anesthetic solution (500 mg/mL), following chemical treatment.

3 | RESULTS AND DISCUSSION

3.1 | Setup of zebrafish embryo infection model

Infection in zebrafish embryos is usually established through microinjection of the bacteria into the embryo. However, this requires specific expertise, expensive equipment, and is time consuming.[30] Therefore, we set up a simple, quick, and cheap *A. baumannii* infection assay based on the immersion of embryos in freshwater with bacteria to bypass the microinjection step. The minimization of the bath volume was also targeted, given the usual scarcity of treatments' quantity needed for assays. This allows to maximize the number of subjects per experiment, which is particularly useful, given the amount of strains tested. Hence, the test was set up in 96-well plates.

Bath immersion was firstly performed on healthy non-dechorionated embryos 6 hpf, by adding 20 µL of TSB with

different bacterial concentrations (10^6, 10^7, and 10^8 CFU/mL) to 180 μL of freshwater. From these initial tests, it was possible to understand that TSB was perhaps toxic to the embryos, given the quick and congruent death observed in all the strains. This would be later confirmed by the next assay, where an additional control with freshwater and the corresponding previous concentrations of the bacteria media was added, without the bacteria, resulting once again in uniform death. It was hypothesized that the component of the TSB responsible for the death was the digest pancreatic of casein.

Two resuspension steps of the bacteria in freshwater (already described in the materials and methods section) were performed before exposure to avoid the toxicity observed with TSB (data not shown).

Firstly, bath immersion was initially performed on tail-injured embryos at 2 days post-fertilization (dpf). By this developmental stage, the mouth is not yet open; therefore, only an injury would be able to provide an easier path for the bacteria to enter the embryo.[30,34] Different concentrations of the *A. baumannii* strains were used with one embryo per well in 96-well plates (10^9 and 10^8 CFU/mL). Viability of embryos was followed for 72 h. In contrast to the healthy embryos, mortality on the exposed tail-injured embryos was observed, in almost every strain tested. The surviving embryos in every strain would often show an affected swimming pattern (side swimming) that was postulated as most likely associated with the delay of the tail regeneration, possibly associated with necrosis of the infected tail end. Additionally, the deficient regeneration of the tail would often lead to a tilted tail malformation on the infected embryos and pericardial edema, as well as abnormalities in the yolk absorption (Figure S1). This was not detected in the tail-injured control embryos, which had already successfully fully regenerated their tails after 24 hpi (data not shown).

Heat-killed and ethanol-killed bacteria controls did not affect the zebrafish embryonic development, neither presented the malformations described.[40] These data likewise reveal that living bacterial cells are required for *A. baumannii* pathogenesis in zebrafish. The above results could corroborate the establishment of *A. baumannii* infection in the zebrafish embryos.

3.2 | Assessment of the virulence of different capsules of *A. baumannii*

To determine the virulence of the different strains, tail-injured embryos were exposed to 10^9 CFU/mL initial inoculum. Figure 1A shows the embryos' survival curve for each strain, and respective control, where no bacteria were added. For better understanding of the survival curves, a table containing the media survival percentage per strain in each observed time was added (Figure 1B). From the survival curve analysis, it was firstly possible to establish a virulence hierarchy, where K44 stain is perceived as an avirulent strain, being non-significantly different from the control. Yet, a study with more subjects involved could possibly differentiate statistically this strain from the control as a

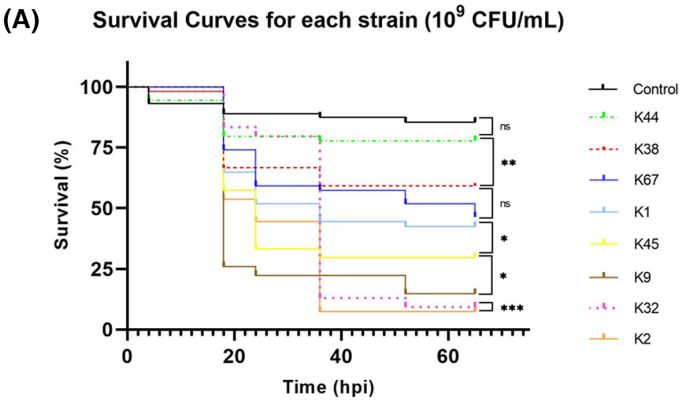

(B)

Time (hpi)	Medium survival percentage per strain at 10^9 CFU/ml (%)								
	K1	K2	K9	K32	K38	K44	K45	K67	Control
0	100	100	100	100	100	100	100	100	100
4	100	100	98.15	98.15	100	94.44	100	100	93.06
18	64.82	53.70	25.93	83.33	66.67	79.63	74.07	74.07	88.90
24	51.85	44.44	22.22	79.63	66.67	79.63	59.26	59.26	88.90
36	44.44	7.41	22.22	12.96	59.26	77.78	57.41	57.41	87.50
52	42.52	7.41	14.82	9.26	59.26	77.78	51.85	51.85	85.42
65	42.52	7.41	14.82	9.26	59.26	77.78	46.30	46.30	85.42

FIGURE 1 Survival curves of each strain. (A) is depicted the survival curves acquired for each strain: in dotted green K44, in dotted red K38, in blue K67, in light blue K1, in yellow K45, in brown K9, in dotted pink K32, and in orange K2. The presented order matches the established virulence hierarchy. Black represents the freshwater control, where no bacteria were added. (B) represents the media survival percentage obtained in each time stamp for all the strains and controls. ns, non-significant; *$p \leq .05$; **$p \leq .01$, ***$p \leq .001$.

tendency to decrease viability is observed. Notwithstanding, K38, K67, and K1 strains, being non-significantly different from one another, stand as the less virulent ones. The K45 strain appears next, followed by K9, the third most virulent studied strain. Lastly, K2 and K32 strains clearly stand out as the most virulent strains, leaving less than 10% of embryo survival. Nevertheless, K2 is significantly more virulent than K32, leading to higher and quicker mortality in the exposed embryos. When comparing to Nogaret et al. (2020), where a similar mode of infection was applied with *P. aeruginosa*, the time point when most of the death occurred was similar (18 hpi). However, for Al-Zubidi, M et al. (2019) where microinjection was used for the *Enterococcus faecalis* infection, death occurred mainly at 40 hpi, which is probably associated with the less virulent pathogen.

Additional data based on a single-point analysis are shown in Table S1. Accordingly, the table displays the final survival percentage with 95% confidence interval of each strain. These data only take into account the final survival percentage, not considering, for instance, how quickly each bacterium was able to kill the subjects. However, the hazard ratio (also with 95% confidence interval) and the median survival, likewise depicted in Table S1, take the evolution of death into account. The hazard ratio is a measurement that compares a given condition A with a condition B and through a ratio expresses how much more dangerous condition A is than condition B. In the table below, the hazard ratio compares each strain (Condition A) with the control with only freshwater (Condition B). Additionally, the median survival is able to give a simple perception of how quickly each pathogen acts, expressing how long each strain takes to kill half of the population.

When evaluating the final survival percentage, bearing in mind the confidence intervals, K2, K9, and K32 strains are the top virulent strains, in no particular order. K45 strain could be as virulent as K2 and K9 strains, or as virulent as K1 and K67, the middle virulent strains, alongside with K38 strain. K44 was once again the only strain where no differences were noticed when compared to the control. Yet, when analyzing the hazard ratios, once again considering the confidence intervals, all the strains except K44, are significantly more hazardous than the control, but there was no difference amongst each other. At last, when analyzing the median survival, K9 is the most virulent strain, killing half the population the fastest, followed by K2 and K45 strains. K1 and K32 strains come next, followed by K67. The remaining strains, K38 and K44, were not capable of killing half of the population.

Through the combined analysis of the survival curves of Figure 1A and the additional data that Table S1 provides, it is implied that K44 is the less virulent studied strain. However, the malformations described above were present in around 30% of the survivor individuals of this strain, versus 5% in the controls, which could indicate that although no significant mortality was calculated, the infection could have been established. As a final point, it was agreed that the model was undoubtedly capable of stating the most virulent strains (K2, K32, K9, and K45) and even defining a hierarchy (K2 > K32 > K9 > K45 > K1 > K67, and K38 > K44).

3.3 | Treatment setup

Bath immersion technique was chosen as the exposure route. To more closely replicate human infections, the inoculum with the bacteria had to be removed and the exposed embryo carefully washed and transferred to a new 96-well plate, before the treatment administration. With this in mind, the treatment timing (and previous suspended bacteria removal) would also have to be optimized: the infection time would have to still lead to significant death in the controls where no treatment was applied (inoculum removed at the given time, and exchanged by freshwater) but at the same time be in time to allow an efficient treatment.

Most of the deaths occurred until 18 hpi; thus, the inoculum removal was tested at 2, 4, 8, 10, and 12 hpi. The experiments allowed to define 12 hpi as the one conceivable treatment time, since shorter exposure would lead to no significant death in any strain when compared with the controls. As far as one can tell, treatment administration had never been performed this late, and later treatments would most likely limit the survival.[41] Consequently, 12 hpi was picked as the treatment timing (and bacterial suspension removal, consequently). This timing was able to lead to significant death for the top four most virulent strains. However, for K1, K38, and K67 strains, no significant death was obtained when shortening the bath exposure to 12 h (Figure S2A–C, respectively). Figure S2D shows the medium survival of the embryos after a 12-h exposure, without treatment versus the survival without the exposure. From its analysis, it is possible, once again to understand that no significant differences were noted, therefore, the treatment would be impossible to test for these strains in these conditions. A deeper analysis through the hazard ratio (Table S2) obtained with the Log-rank (Mantel-Cox) test corroborates that it would be meaningless to test the treatment of K1 strain, K67, and K38, in the previously defined conditions, which worked for the majority of the tested strains. Hence, these strains were left out for the following experiments, given the lack of time to personalize the optimization of the treatment setup based on strains. It is also important to clarify that K44 was excluded from this study since it was not able to lead to significant death even within the full-time exposure.

There was no literature that guided the phage treatment dosage, since all the previous phage treatments that

resorted to the zebrafish embryo model were administered through microinjection, and quantified through its multiplicity of infection (MOI, up to 20).[35,36] Hence, the high dosage of 10^9 PFU/mL was picked, based on the initial bacterial concentration, to ensure high chances of treatment, since it was determined that only sensibly 10^4 CFU/mL were effectively in the embryos (data not shown).

3.4 | Validation of the bath infection model to test efficacy of phage treatments

Another major goal of the present work was to address the relevance of the bath infection model to evaluate the ability of the protocol of bath infection of injured embryos to test the previously produced anti-virulence compounds in vivo. Phages had previously been evaluated in an animal model, including the zebrafish embryo. However, this was the first time these particular k-types would be tested in the zebrafish embryo model.[35,36]

In each experiment, 18 embryos were tested with a single treatment. Three main controls were applied: (1) the embryo with the treatment without any bacterial exposure to ensure that the treatment was not toxic to the embryo, (2) the embryo exposed to the strain for 12 h, and then removed to prove that without the treatment, the infection would lead to greater death, and (3) the embryo with just freshwater to assess the normal mortality associated with the full

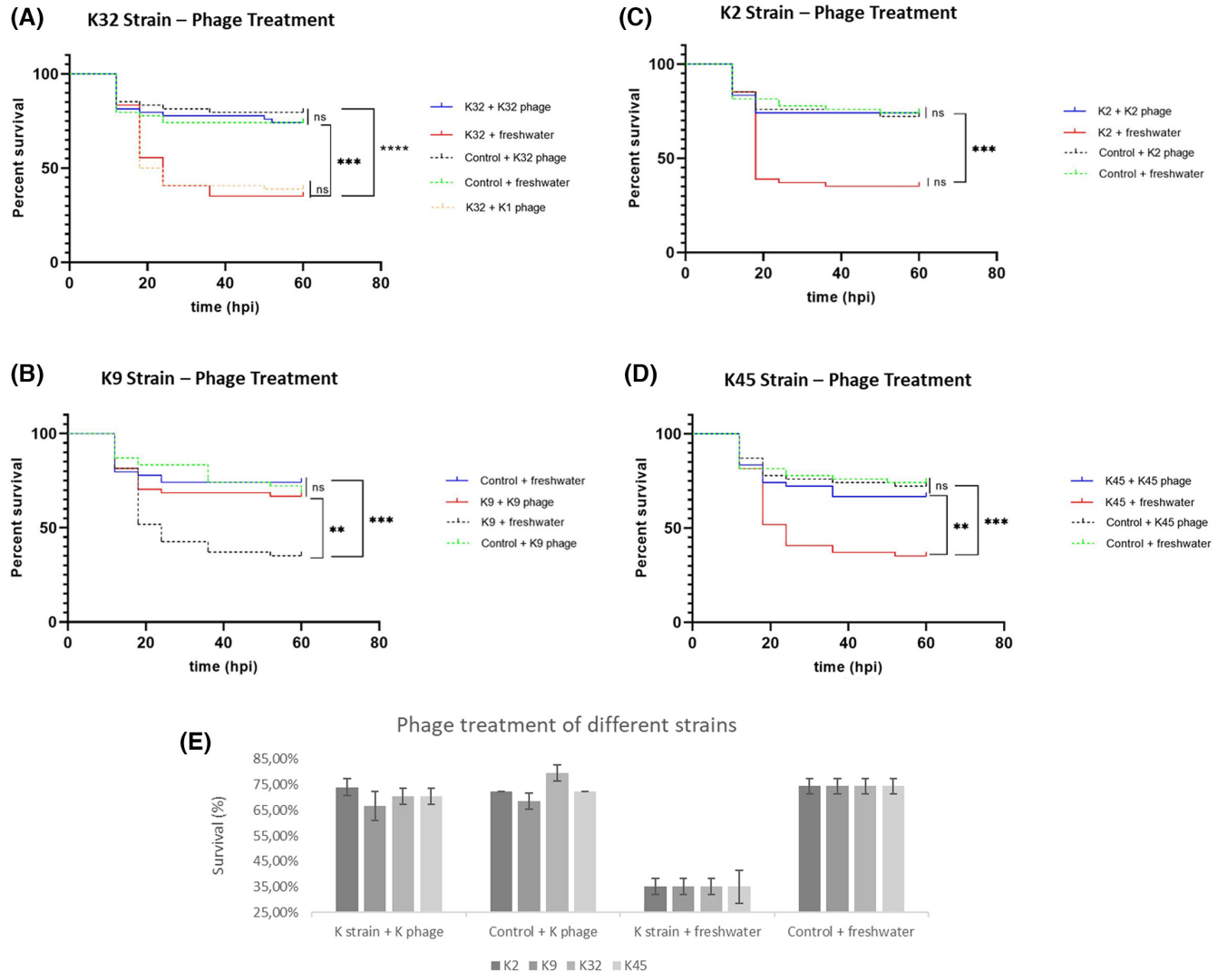

FIGURE 2 Survival curves of the strains treated with phages. In (A) K32, (B) K2, (C) K9, and (D) K45 strain, the blue line shows the survival curve of each strain when the respective phage treatment was applied, while the red line shows the survival curve of each strain, when at 12 hpi the inoculum was replaced with freshwater, whereas the black dotted line shows the survival curve of not exposed individuals, treated with the phage solution, and finally the green line represents the survival of subjects that were not exposed to bacteria, being treated with freshwater. In (E), the medium survival and standard deviations for each condition are depicted, after $n = 3$ independent experiments; ns, non-significant; *$p \leq .05$; **$p \leq .01$, ***$p \leq .001$, ****$p \leq .0001$.

procedure. An additional control was made for one strain role model, K32, where an unspecific treatment based on a phage nonspecific to that strain (K1 Phage), to prove the specificity of the used phage. Additionally, drop tests of the treatments were made by the end of the experiment to ensure that the treatments were active during all the processes.

The phage treatment was efficient for all the tested strains, being able to increase the average survival from 35.19% to up to 74.07% (K32 strain). All the phages performed equally well. The treatment's efficiency depicted in the survival curves is represented in Figure 2A (K32 strain phage treatment), Figure 2B (K2 strain phage treatment), Figure 2C (K9 strain phage treatment), and Figure 2D (K45 strain phage treatment), obtained resorting to the Log-rank (Mantel-Cox) statistical analysis. Figure 2E shows the medium survival and standard deviations of the embryos after a 12-h exposure in all the conditions based on three independent experiments, where the treatment success can also be observed.

From the analysis of Figure 2, it is possible to comprehend that the phage treatment was able to significantly increase the survival of the exposed embryos, particularly significantly when applied to the most virulent strain, K32. Results from K32 strain + K1 phage control (Figure 2A), furthermore, corroborate that only the specific phage is efficient in the treatment of the embryos infected with a particular strain. Altogether, zebrafish embryo bath infection model was capable of validating the phage treatment.

4 | CONCLUSIONS

In this study, bath immersion infection technique carried out in tail-injured embryos was validated to test virulence of bacterial strains and efficiency of treatments. K2, K32, K9, and K45 were the most virulent strains, while K44 was demonstrated as the less virulent one. Phages K2, K9, K32, and K45 were able to significantly save the embryos. Collectively, the overall results implied that the tail-injured zebrafish embryo bath infection model is robust enough to assess virulence, as well as subsequently validating different treatments, while conveying important advantages when compared with other animal models.

There are many research opportunities arising from this study that could be further considered in the future. The perceived malformations in the zebrafish embryos could be explored resorting to more replicates in order to understand the main phenotype changes the infection promotes.

Beyond virulence assessment of the *A. baumannii* strains, the high specificity of phage treatments for a given k-type demands epidemiological studies in order to determine which k-types are more prevalent in human clinical isolates. Merely with this knowledge, the anti-virulence therapy based on phages could be clinically practicable, potentially becoming a viable alternative to present antibacterial treatments through cocktails that included the therapy not only for the most virulent strains but also the most common. More complex and forward-thinking perspectives include proceeding to test the treatments in a more complex animal model and later questioning how the administration would be performed in humans.

AUTHOR CONTRIBUTIONS

Conceptualization, Hugo Oliveira and Begoña Espiña; methodology, Hugo Oliveira, Ana Vieira, and Begoña Espiña; validation, Hugo Oliveira and Begoña Espiña; formal analysis, Sofia Neto; investigation, Sofia Neto and Ana Vieira; resources, Hugo Oliveira and Begoña Espiña; data curation, Sofia Neto, Hugo Oliveira, and Begoña Espiña; writing—original draft preparation, Sofia Neto; writing—review and editing, Sofia Neto, Hugo Oliveira, and Begoña Espiña; supervision, Ana Vieira, Hugo Oliveira, and Begoña Espiña; project administration Hugo Oliveira and Begoña Espiña; funding acquisition, Hugo Oliveira and Begoña Espiña. All authors have read and agreed to the published version of the manuscript.

ACKNOWLEDGMENTS

The authors acknowledge the support from Ivone Pinheiro and Sofia Azevedo in the zebrafish culturing and breeding and from Alejandro Garrido-Maestu in the *A. baumannii* culture and quantification methodology. B.E. acknowledges the financial support of the project SbDtoolBox—Nanotechnology-based tools and tests for Safer-by-Design nanomaterials, with the reference n° NORTE-01-0145-FEDER-000047, funded by Norte2020—North-Regional Operational Programme under the PORTUGAL 2020 Partnership Agreement through the European Regional Development Fund (ERDF).

DISCLOSURES

The authors declare that they have no conflicts of interest.

DATA AVAILABILITY STATEMENT

The authors confirm that the data supporting the findings of this study are available within the article and its Supplementary Material. Raw data of this study are available upon reasonable request.

ORCID

Hugo Oliveira https://orcid.org/0000-0001-9564-5714

REFERENCES

1. Montefour K, Frieden J, Hurst S, et al. *Acinetobacter baumannii*: an emerging multidrug-resistant pathogen in critical care. *Crit Care Nurse*. 2008;28(1):15-26.

2. Sebeny PJ, Riddle MS, Petersen K. *Acinetobacter baumannii* skin and soft-tissue infection associated with war trauma. *Clin Infect Dis*. 2008;47(4):444-499.
3. Wong D, Nielsen TB, Bonomo RA, Pantapalangkoor P, Luna B, Spellberg B. Clinical and pathophysiological overview of Acinetobacter infections: a century of challenges. *Clin Microbiol Rev*. 2017;30:409-447.
4. Murray CJ, Ikuta KS, Sharara F, et al. Global burden of bacterial antimicrobial resistance in 2019: a systematic analysis. *Lancet*. 2022;399:629-655.
5. Santajit S, Indrawattana N. Mechanisms of antimicrobial resistance in *Pasteurellaceae*. *PBioMed Res Int*. 2016;2016:1-8.
6. Tal-Jasper R, Katz DE, Amrami N, et al. Clinical and epidemiological significance of carbapenem resistance in *Acinetobacter baumannii* infections. *Antimicrob Agents Chemother*. 2016;60:3127-3131.
7. Bonnin RA, Cuzon G, Poirel L, Nordmann P. Multidrug-resistant *Acinetobacter baumannii* clone, France. *Emerg Infect Dis*. 2013;19(5):822-823.
8. Qureshi ZA, Hittle LE, O'Hara JA, et al. Colistin-resistant *Acinetobacter baumannii*: beyond carbapenem resistance. *Clin Infect Dis*. 2015;60(9):1295-1303.
9. Fournier P-E, Vallenet D, Barbe V, et al. Comparative genomics of multidrug resistance in *Acinetobacter baumannii*. *PLoS Genet*. 2006;2(1):e7.
10. Tacconelli E, Magrini N. *Global Priority List of Antibiotic-Resistant Bacteria to Guide Research, Discovery, and Development of New Antibiotics*. WHO Press; 2017:1-7.
11. Lin YM, Shin KS, Kim J. Distinct antimicrobial resistance patterns and antimicrobial resistance-harboring genes according to genomic species of Acinetobacter isolates. *J Clin Microbiol*. 2007;45(3):902-905.
12. Geisinger E, Isberg RR. Antibiotic modulation of capsular exopolysaccharide and virulence in *Acinetobacter baumannii*. *PLoS Pathog*. 2015;11:1-27.
13. Russo TA, Luke NR, Beanan JM, et al. The K1 capsular polysaccharide of *Acinetobacter baumannii* strain 307-0294 is a major virulence factor. *Infect Immun*. 2010;78(9):3993-4000.
14. Lees-Miller RG, Iwashkiw JA, Scott NE, et al. A common pathway for O-linked protein-glycosylation and synthesis of capsule in *Acinetobacter baumannii*. *Mol Microbiol*. 2013;89:816-830.
15. Harding CM, Hennon SW, Feldman MF. Uncovering the mechanisms of *Acinetobacter baumannii* virulence. *Nat Rev Microbiol*. 2018;16:91-102.
16. Saipriya K, Swathi CH, Ratnakar KS, Sritharan V. Quorum-sensing system in *Acinetobacter baumannii*: a potential target for new drug development. *J Appl Microbiol*. 2020;128:15-27.
17. Hsieh PF, Lin HH, Lin TL, Chen YY, Wang JT. Two T7-like bacteriophages, K5-2 and K5-4, each encodes two capsule depolymerases: isolation and functional characterization. *Sci Rep*. 2017;7:1-13.
18. Oliveira H, Costa AR, Ferreira A, et al. Functional analysis and antivirulence properties of a new depolymerase from a myovirus that infects *Acinetobacter baumannii* capsule K45. *J Virol*. 2019;93:1-16.
19. Oliveira H, Mendes A, Fraga AG, et al. K2 capsule depolymerase is highly stable, is refractory to resistance, and protects larvae and mice from *Acinetobacter baumannii* sepsis. *Appl Environ Microbiol*. 2019;85:e00934-19.
20. Wyres KL, Cahill SM, Holt KE, Hall RM, Kenyon JJ. Identification of *Acinetobacter baumannii* loci for capsular polysaccharide (KL) and lipooligosaccharide outer core (OCL) synthesis in genome assemblies using curated reference databases compatible with Kaptive. *Microb Genomics*. 2020;6:e000339.
21. Sulakvelidze A, Alavidze Z, Morris J. Bacteriophage therapy. *Antimicrob Agents Chemother*. 2001;45:649-659.
22. Harada LK, Silva EC, Campos WF, et al. Biotechnological applications of bacteriophages: state of the art. *Microbiol Res*. 2018;212–213:38-58.
23. Mason KA, Losos JB, Singer SR, Raven PH, Johnson GB. Biology. 8th ed. McGraw-Hill; 2011.
24. Schooley RT, Biswas B, Gill JJ, et al. Development and use of personalized bacteriophage-based therapeutic cocktails to treat a patient with a disseminated resistant *Acinetobacter baumannii* infection. *Antimicrob Agents Chemother*. 2017;61:e00954-17.
25. Popova AV, Shneider MM, Arbatsky NP, et al. Specific interaction of novel *Friunavirus* phages encoding tailspike depolymerases with corresponding *Acinetobacter baumannii* capsular types. *J Virol*. 2021;95:1714-1734.
26. Domingues R, Barbosa A, Santos SB, et al. Unpuzzling friunavirus-host interactions one piece at a time: phage recognizes *Acinetobacter pittii* via a new k38 capsule depolymerase. *Antibiotics*. 2021;10:1304.
27. Popova AV, Lavysh DG, Klimuk E, et al. Novel Fri1-like viruses infecting *Acinetobacter baumannii*—vB_AbaP_AS11 and vB_AbaP_AS12—characterization, comparative genomic analysis, and host-recognition strategy. *Viruses*. 2017;9:188.
28. Oliveira H, Costa AR, Konstantinides N, et al. Ability of phages to infect *Acinetobacter calcoaceticus-Acinetobacter baumannii* complex species through acquisition of different pectate lyase depolymerase domains. *Environ Microbiol*. 2017;19:5060-5077.
29. Lieschke GJ, Currie PD. Animal models of human disease: zebrafish swim into view. *Nat Rev Genet*. 2007;8:353-367.
30. Pont S, Blanc-Potard AB. Zebrafish embryo infection model to investigate *Pseudomonas aeruginosa* interaction with innate immunity and validate new therapeutics. *Front Cell Infect Microbiol*. 2021;11:1-11.
31. Strähle U, Scholz S, Geisler R, et al. Zebrafish embryos as an alternative to animal experiments—a commentary on the definition of the onset of protected life stages in animal welfare regulations. *Reprod Toxicol*. 2012;33:128-132.
32. Bhuiyan MS, Ellett F, Murray GL, et al. *Acinetobacter baumannii* phenylacetic acid metabolism influences infection outcome through a direct effect on neutrophil chemotaxis. *Proc Natl Acad Sci U S A*. 2016;113:9599-9604.
33. Kimmel CB, Ballard WW, Kimmel SR, Ullmann B, Schilling TF. Stages of embryonic development of the zebrafish. *Dev Dyn*. 1995;203:253-310.
34. Nogaret P, El Garah F, Blanc-Potard AB. A novel infection protocol in zebrafish embryo to assess *Pseudomonas aeruginosa* virulence and validate efficacy of a quorum sensing inhibitor in vivo. *Pathogens*. 2021;10:401.
35. Al-Zubidi M, Widziolek M, Court EK, et al. Identification of novel bacteriophages with therapeutic potential that target *Enterococcus faecalis*. *Infect Immun*. 2019;87:e00512-19.
36. Cafora M, Deflorian G, Forti F, et al. Phage therapy against *Pseudomonas aeruginosa* infections in a cystic fibrosis zebrafish model. *Sci Rep*. 2019;91(9):1-10.

37. Nemec A, Krizova L, Maixnerova M, et al. Genotypic and phenotypic characterization of the *Acinetobacter calcoaceticus-Acinetobacter baumannii* complex with the proposal of *Acinetobacter pittii* sp. nov. (formerly Acinetobacter genomic species 3) and *Acinetobacter nosocomialis* sp. nov. (formerly Acinetobacter genomic species 13TU). *Res Microbiol*. 2011;162:393-404.
38. Oliveira H, Pinto G, Oliveira A, et al. Characterization and genomic analyses of two newly isolated Morganella phages define distant members among Tevenvirinae and Autographivirinae subfamilies. *Sci Rep*. 2017;7:46157.
39. Organisation for Economic Co-operation and Development (OECD). Guidelines for testing of chemicals. *Dermatotoxicology*. 2013;509-511. doi:10.3109/9781841848570-66
40. Díez-Martínez R, de Paz H, Bustamante N, García E, Menéndez M, García P. Improving the lethal effect of Cpl-7, a pneumococcal phage lysozyme with broad bactericidal activity, by inverting the net charge of its cell wall-binding module. *Antimicrob Agents Chemother*. 2013;57:5355-5365.
41. Blázquez B, Fresco-Taboada A, Iglesias-Bexiga M, Menéndez M, García P. PL3 amidase, a tailor-made lysin constructed by domain shuffling with potent killing activity against pneumococci and related species. *Front Microbiol*. 2016;7:1-13.

SUPPORTING INFORMATION

Additional supporting information can be found online in the Supporting Information section at the end of this article.

How to cite this article: Neto S, Vieira A, Oliveira H, Espiña B. Assessing *Acinetobacter baumannii* virulence and treatment with a bacteriophage using zebrafish embryos. *The FASEB Journal*. 2023;37:e23013. doi:10.1096/fj.202300385R